Available online at www.sciencedirect.com
SCIENCE DIRECT®
Journal of Solid State Chemistry 173 (2003) 425–434
JOURNAL OF SOLID STATE CHEMISTRY
http://elsevier.com/locate/jssc

Crystal structure, phase transitions and ferroelastic properties of $[(CH_3)_2NH_2]_3[Bi_2Cl_9]$

M. Wojtaś,[a] G. Bator,[a] R. Jakubas,[a,*] J. Zaleski,[b] B. Kosturek,[c] and J. Baran[d]

[a] *Faculty of Chemistry, University of Wrocław, Joliot-Curie 14, 50-383 Wrocław, Poland*
[b] *Institute of Chemistry, University of Opole, Oleska 48, 45-951 Opole, Poland*
[c] *Institute of Experimental Physics, University of Wrocław, 9 Max Born Square, 50-204 Wrocław, Poland*
[d] *Institute of Low Temperature and Structure Research of the Polish Academy of Science, Okólna 2, 50-950 Wrocław, Poland*

Received 15 July 2002; received in revised form 19 December 2002; accepted 1 March 2003

Abstract

A sequence of structural phase transitions in $[(CH_3)_2NH_2]_3[Bi_2Cl_9]$ (DMACB) is established on the basis of differential scanning calorimetry (DSC) and dilatometric studies. Four phase transitions are found: at 367/369, 340/341, 323/325 and 285/292 K (on cooling/heating). The crystal structure of DMACB is determined at 350 K. It crystallizes in monoclinic space group $P2_1/n$: $a = 8.062(2)$, $b = 21.810(4)$, $c = 14.072(3)$ Å, $\beta = 92.63(3)^\circ$, $Z = 4$, $R_1 = 0.0575$, w$R_2 = 0.1486$. The crystal is built of the double chain anions (''pleated ribbon structure'') and the dimethylammonium cations. Dielectric studies in the frequency range 75 kHz–900 MHz indicate relatively fast reorientation of the dimethylammonium cations over the I, II, III and IV phases. Infrared spectra are recorded in the temperature range 40–300 K and analyzed in region assigned to the symmetric and asymmetric NC_2 stretching vibrations. Optical observations show the existence of the ferroelastic domain structure over all phases below 367 K. The possible mechanisms of phase transitions are discussed on the basis of presented results.

Keywords: Halogenobismuthate(III); Structure; Phase transition; Ferroelastic

1. Introduction

Crystals belonging to halogenoantimonates(III) and bismuthates(III) of a general formula $R_aM_bX_{(3b+a)}$ (R = organic cations; M = Sb and Bi; X = Cl, Br, I) have attracted much interest because of their ferroelastic and ferroelectric properties and structural phase transitions [1–5]. We focused our attention on crystals with the $R_3M_2X_9$ composition since most of them revealed the electric non-linear properties and were promising from the application point of view. There was found a clear correlation between the crystal structure and physical properties of these compounds. Their anionic $M_2X_9^{3-}$ sublattice is built of:

(i) polyanionic one-dimensional zigzag chains (methylammonium chloride analogues [6]),
(ii) two-dimensional layers (dimethylammonium and trimethylammonium salts [7]),
(iii) discrete bioctahedral anionic units (various alkylammonium iodoantimonates and iodobismuthates [8]).

The second group of crystals (ii) shows considerable importance because of their pyro- and ferroelectric properties. The crystals with the $R_3M_2X_9$ composition frequently undergo numerous solid–solid phase transitions. It was shown that the dynamics of organic cations significantly changes at the phase transition temperatures, pointing out an important role of the cations in the mechanisms of the transitions. The different structural characteristics and various physical properties depend on the size and symmetry of the organic cations as well as of the type of halogen atoms.

In turn, the influence of the metal atoms on properties of compounds was investigated e.g., in the case of $[(CH_3)_3NH]_3[Sb_{2(1-x)}Bi_{2x}Cl_9]$ (TMACAB) mixed crystals [9]. Crystal structure and dielectric relaxation studies of them showed that a substitution of antimony by bismuth led to the disappearance of ferroelectric

*Corresponding author. Fax: +48-71-328-2348.
E-mail address: rj@wchuwr.chem.uni.wroc.pl (R. Jakubas).

0022-4596/03/$ - see front matter
doi:10.1016/S0022-4596(03)00137-3

properties (for $x>0.33$). This was explained in terms of the essential changes in the crystal structure of mixed compounds. It has turned out that for the mixed crystals with $x>0.33$ the anionic sublattice, instead of two dimensional layers, is composed of the discrete $[Sb_{2(1-x)}Bi_{2x}Cl_9^{3-}]$ bioctahedral units. These studies clearly showed that ferroelectricity encountered in either pure dimethylammonium or trimethylammonium analogues, $[(CH_3)_2NH_2]_3[Sb_2Cl_9]$ [10], $[(CH_3)_2NH_2]_3[Sb_2Br_9]$ [11], $[(CH_3)_3NH]_3[Sb_2Cl_9]$ [12]), was strictly connected with the existence of the polyanionic layers. Since pure bismuth analogue—TMACB, in contrast to TMACA, was destitute of both ferroelectricity and layer structure, we could expect the same situation in closely related dimethylammonium analogue—$[(CH_3)_2NH_2]_3[Bi_2Cl_9]$ (DMACB). It seemed interesting to settle the problem of possible polar properties in DMACB. Furthermore, Rajan et al. [13] reported proton magnetic resonance (^{1}H NMR) studies on DMACB. These results indicated the presence of two phase transitions at 152 and 78 K, which were assigned to the changes in the reorientational dynamics of the cation groups. The authors concluded that DMACB, similarly as the closely related antimony compound—DMACA, could be a potential ferroelectric material in the low-temperature region.

The main aim of this paper is to study the physical properties of the pure bismuth analogue, tris(dimethylammonium) nonachlorodibismuthate(III), $[(CH_3)_2NH_2]_3[Bi_2Cl_9]$ (DMACB) and to compare them with those of the pure antimony one, $[(CH_3)_2NH_2]_3[Sb_2Cl_9]$ (DMACA) being a ferroelectric below 243 K. Our intention was, particularly, a verification of the sequence of phase transitions proposed by Rajan et al. [13].

2. Experimental

The powder of tris(dimethylammonium) nonachlorodibismuthate(III) $[(CH_3)_2NH_2]_3[Bi_2Cl_9]$ (DMACB) were obtained by reaction of $(CH_3)_2NH_2Cl$ and $BiCl_3$ in a concentrated hydrochloric acid. The large single crystals of DMACB were grown by a slow evaporation of an aqueous solution.

The single crystal for the X-ray measurements was selected as a mono-domain one at room temperature using the polarizing microscope. After that, temperature was changed very slowly up to 350 K in order to avoid the polydomain state.

The unit cells parameters were obtained from a least-squares refinement of 29 reflections in the 2θ range of 13–24°. Data collections were carried out at 350.0(1) K on a Kuma KM-4-diffractometer equipped in an Oxford Cryosystem cooler. Two standard reflections were monitored every 50 measurements showing that intensity variations were negligible. Lorentz, polarizations and semiempirical absorption corrections were applied. Hydrogen atoms were included using standard geometric criteria and constrained to a distances of 0.90 and 0.96 Å for N–H and C–H, respectively.

KUMA software was used during the data collection, cell refinement and data reduction process [14]. The SHELXS-97 [15] and SHELXL-97 [16] programs were used for structure solution and refinement. The structure drawings were prepared using XP program from the SHELXTL [17]. The details of the data collection and processing are listed in Table 1. Final atomic coordinates and equivalent isotropic displacement parameters for non-hydrogen atoms are shown in Table 2. Bond lengths and angles for anionic sublattice are given in Table 3.

Crystallographic data for the structure reported in this paper (excluding structure factors) have been deposited with the Cambridge Crystallographic Data Centre, CCDC no. 189320 Copies of this information may be obtained free of charge from the Director, CCDC, 12 UNION Road, Cambridge 1EZ UK (fax: +44-1223-336033; e-mail: deposit@ccdc.cam.ac.uk, http://www.ccdc.cam.ac.uk).

The complex electric permittivity, $\varepsilon^* = \varepsilon' - i\varepsilon''$, was measured by a HP 4285A Precision LCR Meter in the frequency range between 75 kHz and 20 MHz and in the temperature range between 100 and 400 K as well as by a HP 4191A Impedance analyser in the frequency range between 30 and 900 MHz and in the temperature range

Table 1
Basic crystallographic data, data collection and refinement parameters for DMACB at 350 K

Temperature	350.0(1) K
Wavelength	0.71073 Å
Empirical formula	$[NH_2(CH_3)_2]_3[Bi_2Cl_9]$
Formula weight	875.29
Crystal system	Monoclinic
Space group	$P2_1/n$ (No. 14)
Unit cell dimensions	$a = 8.062(2)$ Å $b = 21.810(4)$ Å $c = 14.072(3)$ Å $\beta = 92.63(3)^\circ$
Volume	2471.7(9) Å^3
Z, Calculated density	4, 2.352 mg/m^3
Colour	colourless
Shape	plate
Absorption coefficient	15.187 mm^{-1}
$F(000)$	1600
Crystal size	$0.1 \times 0.1 \times 0.2$ mm^3
Range of h, k and l	$0 \to 8$, $0 \to 19$, $-14 \to 14$
Reflections collected/unique	2652/2443 [$R_{int} = 0.0495$]
Refinement method	Full-matrix least-squares on F^2
Data/restraints/parameters	2443/9/182
Goodness-of-fit on F^2	1.023
Final R indices [$I > 2\sigma(I)$]	$R_1 = 0.0575$, w$R_2 = 0.1486$
R indices (all data)	$R_1 = 0.1299$, w$R_2 = 0.1812$
Max. and min. heights in final $\Delta\rho$ map	1.230 and -1.054 eÅ^{-3}

Table 2
Atomic coordinates ($\times 10^4$) and equivalent isotropic displacement parameters ($Å^2 \times 10^3$) for DMACB at 350 K. U_{eq} is defined as one third of the trace of the orthogonalized U_{ij} tensor

	x	y	z	U_{eq}
Bi(1)	2527(1)	1523(1)	887(1)	78(1)
Bi(2)	2318(1)	38(1)	−2493(1)	83(1)
Cl(1)	2688(11)	2130(3)	2431(5)	155(3)
Cl(2)	4790(9)	2191(4)	204(6)	158(3)
Cl(3)	189(10)	2209(4)	208(7)	170(3)
Cl(4)	2347(9)	858(3)	−904(4)	127(2)
Cl(5)	154(9)	742(4)	1759(6)	170(3)
Cl(6)	5137(8)	747(3)	1677(5)	149(3)
Cl(7)	2220(9)	−581(4)	−4040(4)	152(3)
Cl(8)	−34(9)	677(4)	−3259(5)	154(3)
Cl(9)	4466(8)	721(3)	−3210(5)	132(2)
N(1)	−1748(18)	−796(7)	5579(18)	219(15)
C(2)	−3310(2)	−578(12)	5940(2)	235(18)
C(3)	−1890(4)	−1425(8)	5209(18)	222(19)
N(4)	−2780(4)	763(7)	8590(12)	330(2)
C(5)	−2410(4)	552(13)	9562(13)	260(2)
C(6)	−2580(4)	1427(8)	8460(2)	235(19)
N(7)	7100(3)	2312(8)	2374(16)	340(2)
C(8)	7680(6)	2947(9)	2310(3)	490(5)
C(9)	7800(5)	2007(15)	3230(2)	390(4)

between 270 and 360 K. The dimensions of the sample were of the order of $5 \times 3 \times 1\,mm^3$. The overall error for the real and imaginary parts of the complex electric permittivity was less than 5% and 10%, respectively.

Differential scanning calorimetry (DSC) measurements were carried out using a Perkin Elmer DSC-7 in the temperature range 100–400 K.

The dilatometric measurements were performed by a thermomechanical analyser Perkin Elmer TMA-7 in the temperature range 100–400 K. The dimensions of the sample were of the order of $5 \times 3 \times 3\,mm^3$.

Infrared spectra of DMACB (mulls in Nujol) in the temperature range 40–300 K were recorded with FT IR spectrometer BRUKER IFS-88 over the wavenumber range 4000–60 cm^{-1} with a resolution of 1 cm^{-1}. The program GRAMS/386 Galactic Industries was used for numeral fitting of the experimental data.

Table 3
Selected bond lengths (Å) and angles (°) for DMACB at 350 K

Bi(1)–Cl(1)	2.543(7)
Bi(1)–Cl(2)	2.556(7)
Bi(1)–Cl(3)	2.557(7)
Bi(1)–Cl(4)	2.905(6)
Bi(1)–Cl(5)	2.879(7)
Bi(1)–Cl(6)	2.884(6)
Bi(2)–Cl(4)	2.863(6)
Bi(2)–Cl(5)#1	2.849(7)
Bi(2)–Cl(6)#2	2.871(6)
Bi(2)–Cl(7)	2.561(6)
Bi(2)–Cl(8)	2.552(7)
Bi(2)–Cl(9)	2.529(6)
Cl(1)–Bi(1)–Cl(2)	90.9(3)
Cl(1)–Bi(1)–Cl(3)	91.3(3)
Cl(1)–Bi(1)–Cl(4)	178.6(2)
Cl(1)–Bi(1)–Cl(5)	87.3(3)
Cl(1)–Bi(1)–Cl(6)	88.2(2)
Cl(2)–Bi(1)–Cl(3)	93.0(3)
Cl(2)–Bi(1)–Cl(4)	88.1(2)
Cl(2)–Bi(1)–Cl(5)	175.9(2)
Cl(2)–Bi(1)–Cl(6)	87.6(2)
Cl(3)–Bi(1)–Cl(4)	87.8(2)
Cl(3)–Bi(1)–Cl(5)	90.8(3)
Cl(3)–Bi(1)–Cl(6)	179.2(3)
Cl(4)–Bi(1)–Cl(5)	93.8(2)
Cl(4)–Bi(1)–Cl(6)	92.7(2)
Cl(5)–Bi(1)–Cl(6)	88.6(2)
Cl(4)–Bi(2)–Cl(5)#1	94.1(2)
Cl(4)–Bi(2)–Cl(6)#2	94.6(2)
Cl(4)–Bi(2)–Cl(7)	173.1(2)
Cl(4)–Bi(2)–Cl(8)	88.2(2)
Cl(4)–Bi(2)–Cl(9)	87.9(2)
Cl(5)#1–Bi(2)–Cl(6)#2	89.9(2)
Cl(5)#1–Bi(2)–Cl(7)	89.9(2)
Cl(5)#1–Bi(2)–Cl(8)	87.7(2)
Cl(5)#1–Bi(2)–Cl(9)	177.7(2)
Cl(6)#2–Bi(2)–Cl(7)	91.1(2)
Cl(6)#2–Bi(2)–Cl(8)	176.5(2)
Cl(6)#2–Bi(2)–Cl(9)	91.2(2)
Cl(7)–Bi(2)–Cl(8)	86.3(2)
Cl(7)–Bi(2)–Cl(9)	88.1(2)
Cl(8)–Bi(2)–Cl(9)	91.1(2)
Bi(2)–Cl(4)–Bi(1)	171.0(3)
Bi(2)#1–Cl(5)–Bi(1)	175.9(3)
Bi(2)#2–Cl(6)–Bi(1)	178.7(3)

Symmetry transformations used to generate equivalent atoms: #1: $-x,-y,-z$. #2: $-x+1,-y,-z$.

3. Results

3.1. The crystal structure of DMACB

$[(CH_3)_2NH_2]_3[Bi_2Cl_9]$ (DMACB) belongs to a monoclinic $P2_1/n$ space group at 350 K. The independent part of the unit cell contains the $[Bi_2Cl_9^{3-}]$ anion and three independent dimethylammonium cations (Fig. 1). The anionic sublattice of this crystal is built up of the one-dimensional polyanionic chains (ribbon structure) composed of distorted $BiCl_6^{3-}$ octahedra connected with others by corners and extended along the ***a***-axis (see Fig. 2). In each octahedron there are three terminal and three bridging Bi–Cl bonds. Each bridging chlorine is located opposite to the terminal Cl atom.

The Bi–Cl bond lengths are between 2.529(6) and 2.905(6) Å. They fall into two well-defined ranges. Shorter lengths, between 2.529(6) and 2.557(7) Å, are characteristic of terminal bonds, whereas longer ones, between 2.849(7) and 2.905(6) Å, of bridging bonds. In comparison to bond lengths observed in other structures of halogenobismuthates(III) the terminal as well as bridging bonds are only very slightly distorted from the mean values.

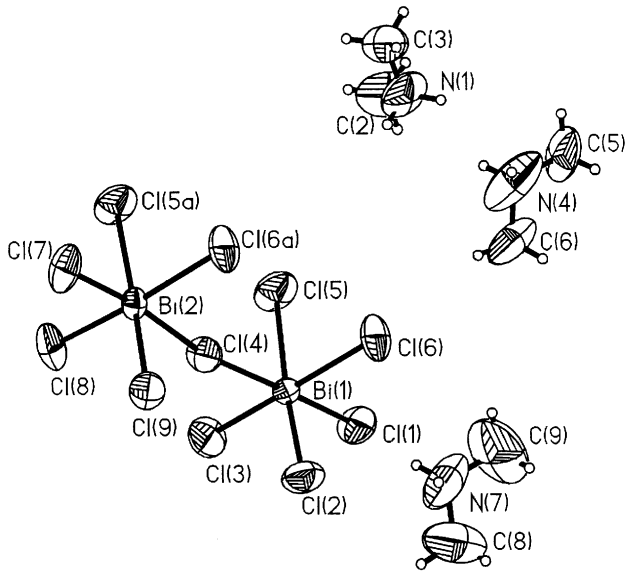

Fig. 1. Atom numbering of DMACB.

The Cl–Bi–Cl angles *cis* to each other are between 86.3(2) and 94.6(2)°. The Bi–Cl–Bi angles are between 171.0(3)° and 178.7(3)°. The packing of the unit cell, almost along the ***a*** direction is presented in Fig. 3. The cations are shown with isotropic temperature factors for clarity.

The co-ordination geometry of the $[Bi_2Cl_9^{3-}]$ species is close to regular bioctahedral with little evidence of a stereochemically active bismuth(III) lone pair (in terms of bond length or angular distortions [18]).

The alkylammonium cations are located between anions and connected to the halogen atoms by weak N–H···Cl hydrogen bonds. The parameters of those hydrogen bonds are shown in Table 4. The C and N atoms are characterized by relatively large thermal ellipsoids. Attempts of the splitting of their positions were not successful. One can suggest, however, two types of possible reorientations of all DMA cations in this phase: (a) reorientation about their diad axis (C_2

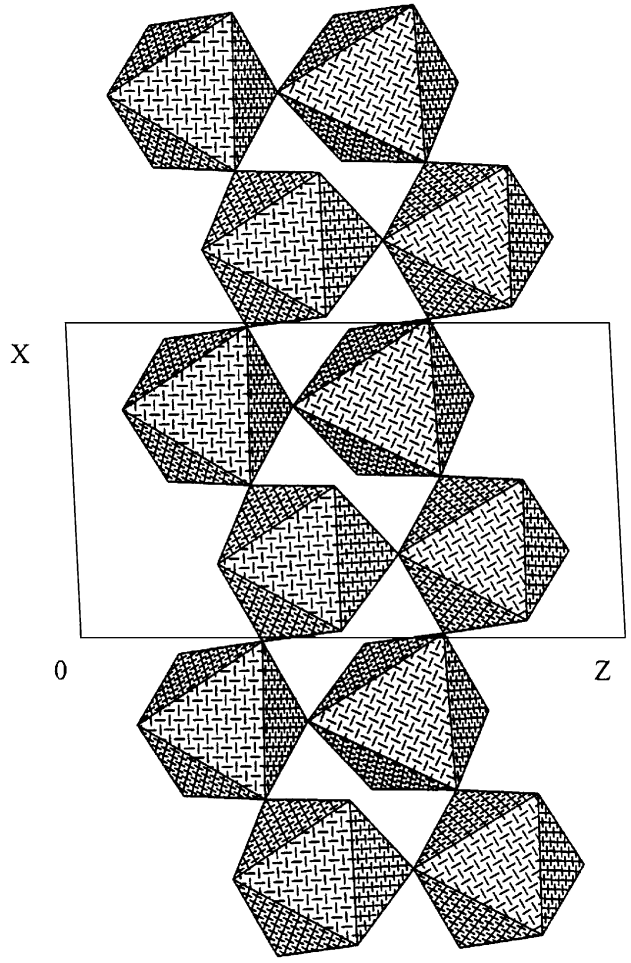

Fig. 2. The one-dimensional double chain of the anionic sublattice as a polyhedral representation.

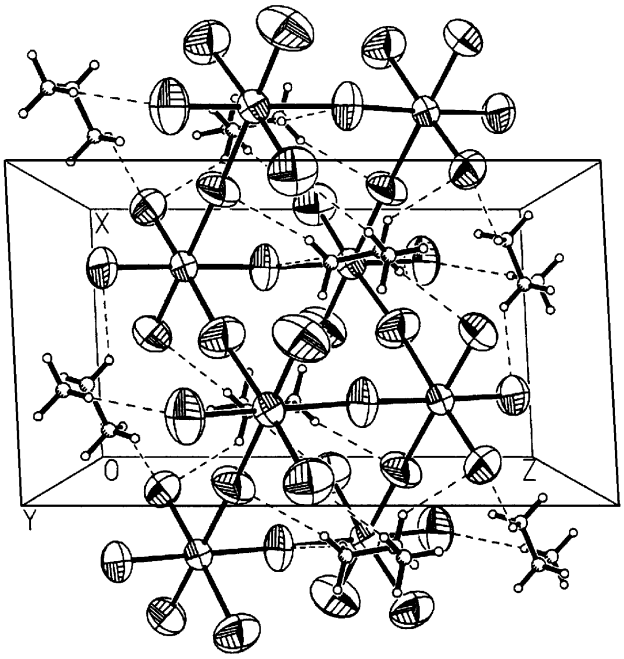

Fig. 3. Perspective view of the crystal structure of DMACB along the ***b***-axis.

Table 4
Hydrogen bonding system of DMACB distances (Å) and angles (°) at 350 K

	N–H	H···Cl	N···Cl	N–H···Cl
N(1)–H(1A)···Cl(7[a])	0.90	2.57	3.25	133
N(4)–H(4A)···Cl(9[b])	0.90	2.61	3.29	134
N(4)–H(4B)···Cl(8[a])	0.90	2.75	3.50	140
N(7)–H(7B)···Cl(1)	0.90	2.75	3.59	156

[a] Symmetry code: x, y, $z+1$.
[b] Symmetry code: $x-1$, $z+1$.

motion), (b) reorientation about an axis parallel to the C–C direction. We should remember that the (b) type of motion was found in the ferroelectric crystals DMACA and DMABA in the disordered paraelectric phases [19]. The isotropic rotation of DMA cations should be, therefore, excluded over all the monoclinic phases.

We tried to determine the crystal structure of DMACB at 300 K—phase IV. We did not succeed in the solution of the crystal structure. The results indicate, however, that DMACB at 300 K appears to be in incommensurate phase. The lattice parameters of the unit cell of the average structure (the monoclinic symmetry—$P2_1/n$) are as follows: $\boldsymbol{a} = 8.024(1)$, $\boldsymbol{b} = 21.758(1)$, $\boldsymbol{c} = 42.211(2)$ Å, $\boldsymbol{\beta} = 93.82(1)^\circ$. For one of the intermediate phase (phase III at 330 K) the following parameters were found $\boldsymbol{a} = 8.044(1)$, $\boldsymbol{b} = 21.739(1)$, $\boldsymbol{c} = 14.046(1)$ Å, $\boldsymbol{\beta} = 93.23^\circ$, but it is difficult to confirm that the incommensurate phase exists. Decrease of the temperature below 285 K leads to a splitting of reflections, which suggests that below 285 K the crystal transforms into a triclinic phase. The lack of pyroelectric effect suggests the presence of centrosymmetric space group $P\bar{1}$.

3.2. Thermal behavior of DMACB

Fig. 4 shows DSC runs on cooling and heating (at the rate of 5 K/min) for DMACB. The calorimetric measurements clearly show an existence of four solid–solid reversible phase transitions. Temperatures and entropies of the corresponding phase transition are shown in Table 5. The lowest temperature phase transition (IV–V) clearly of first order type, accompanied by the largest entropy change ($\Delta S = 3.5$ J/mol K) may be classified as an order–disorder type. The remaining three transitions,

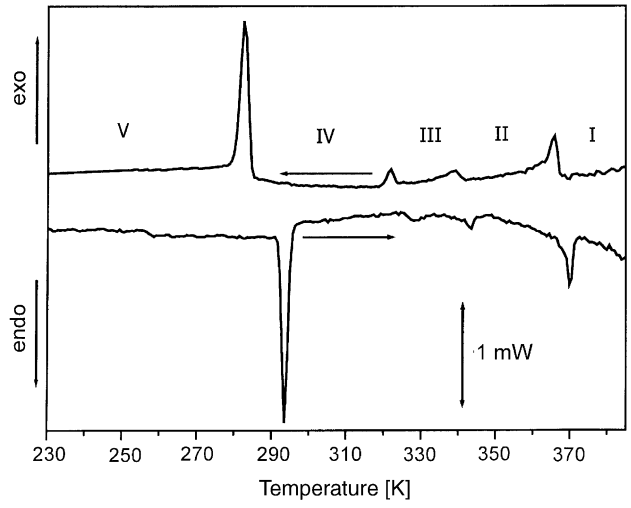

Fig. 4. DSC curves obtained on heating–cooling for DMACB (scanning rate 5 K/min, sample mass 12.01 mg.)

Table 5
Structural phase transitions in DMACB detected by the DSC measurements

Phase transition	T_c (cooling/heating) (K)	ΔS (J mol^{-1} K^{-1})
I→II	367/369	0.84
II→III	340/341	0.27
III→IV	323/325	0.26
IV→V	285/292	3.49

T_c and ΔS stand for transition temperature (taken during cooling/heating) and entropy of the phase transition, respectively.

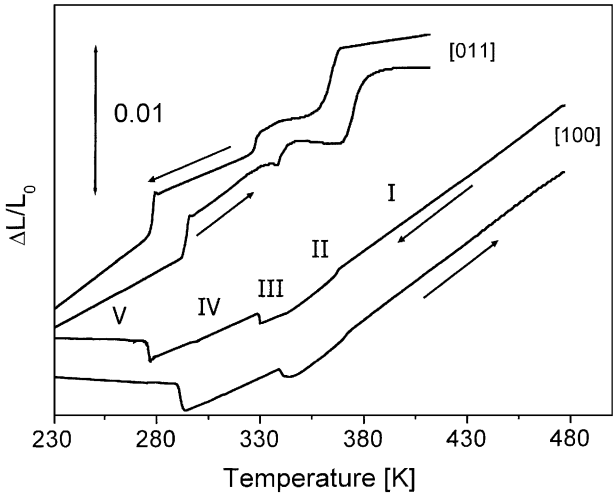

Fig. 5. Temperature dependence of the linear thermal expansion $\Delta L/L_0$ along the [100] and [011] directions for the DMACB crystals.

taking into account the value of the temperature hysteresis, are considered as weak discontinuous transitions. In turn the entropy effects accompanying these transitions are quite small pointing out their displacive nature.

Fig. 5 shows the results on the linear thermal expansion, $\Delta L/L_0$. The measurements were carried out on virgin samples of crystal, which were in the shape of long flattened needles. The ***a***-axis corresponds to the direction along the needle and the direction perpendicular to the ***a***-axis and to the biggest plate of the crystal corresponds to direction [011]. The DMACB crystals are quite fragile, thus the attempts of cutting the samples along other directions failed.

We can state that the dilatometric results are in a good agreement with those obtained from DSC measurements. Dependence of $\Delta L/L_0$ versus temperature shows four anomalies corresponding to four phase transitions found by the DSC technique. Three of them are seen as stepwise changes in dimensions of the crystal sample, whereas the II–III transition is accompanied by a change in the temperature coefficient of thermal dilation $\alpha = \Delta L/(\Delta T * L_0)$. It should be

emphasized that both the calorimetric and dilatometric measurements presented in this paper do not detect any phase transition around 152 K suggested by Rajan et al. [13].

It is interesting that non-polar mixed DMACAB crystals for $0.17<x<0.41$ are characterized by quite different sequence of phase transitions in comparison to that of pure bismuth analogue—DMACB. In spite of the fact that the both types of these crystals have the same polyanionic structure, dynamics of dimethylammonium cations determining the phase transition sequence is quite different (see Fig. 7 in [21]).

3.3. The dielectric properties

The results of dielectric measurements obtained for samples cut perpendicularly to the (011) plane are presented in Fig. 6. The real part of the complex electric permittivity vs. temperature curve, $\varepsilon'(T)$, exhibits four anomalies at temperatures corresponding to the phase transitions found by the DSC and dilatometric technique in DMACB. Two higher temperature phase transitions (at 367 and 340 K) appear only as subtle inflexions on the ε' curve. Over the phase I one can observe a clear divergence in the ε' value between 75 kHz and 5 MHz. This is probably caused by an influence of the electric conductivity, which is supported by the shape of the temperature dependence of the dielectric losses, ε'' vs. temperature (inset in Fig. 6).

The electric permittivity at the IV→V transition falls abruptly from 17.5 to 15 ($\Delta\varepsilon = 2.5$). The step-wise change in the ε' value indicate that we deal with a freezing of rotational motion of dipolar groups.

Since the phase IV revealed the feature of a plastic-like one, taking into account the dielectric response, we should observe the dielectric dispersion and absorption

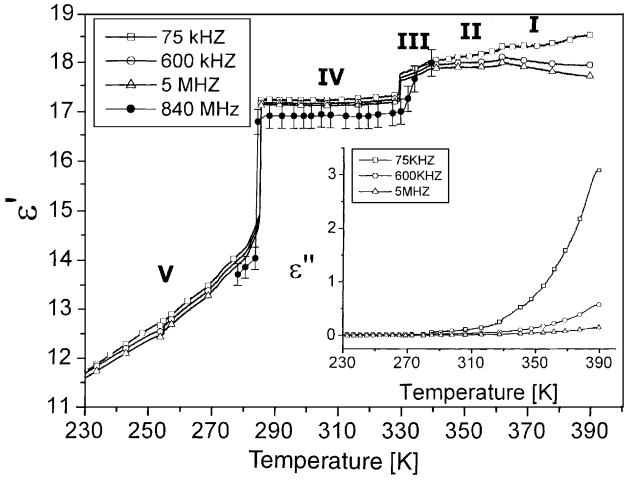

Fig. 6. Temperature dependence of $\varepsilon'_{[011]}$ (main figure) and $\varepsilon''_{[011]}$ (inset) between 75 kHz and 840 MHz for DMACB crystals.

in the frequency region corresponding to the characteristic dielectric relaxation time for a rotation of dipolar group. In order to check if any relaxation process appears at higher frequencies we performed the measurements of the complex electric permittivity, $\varepsilon^* = \varepsilon' - i\varepsilon''$, in the frequency range between 30 and 900 MHz. The results of the temperature dependence of the ε' at selected frequency (840 MHz) are presented in Fig. 6. No dielectric losses were observed in this frequency region, so we can state that no dielectric relaxation process is present for DMACB crystals below 900 MHz. It means that the dielectric relaxation should appear at higher frequencies. This supposition is in agreement with the dielectric results obtained for DMACA, which is a classical example of ferroelectric with an order–disorder mechanism. Such crystals are characterized by an existence of a critical slowing down of the macroscopic relaxation process, which manifests itself as a shift of the dielectric absorption towards the megahertz frequency range. Since in DMACB the dipole–dipole long-range interactions are negligible it seems reasonable to assume that the dynamics of cations is relatively fast.

3.4. The optical observations

The observations of ferroelastic domain structure were carried out between 250 and 400 K. The detail analysis was performed, however, for the room temperature phase, i.e. phase IV. There are three types of domains in phase IV (see Fig. 7). Two of them differ by an orientation of the refractive index indicatrix. The axes of indicatrix are inclined by an angle of 25° to the ***a***-direction. These domains belong undoubtedly to the monoclinic symmetry. Moreover the optical observations point to the fact that the DMACB crystal is optically negative, i.e. $n_\alpha > n_\gamma > n_\beta$. On the other hand in third type of domains the angle between an indicatrix axis and crystallographic ***a***-axis is equal to 0. This state is most probably connected with an existence of a higher symmetry phase. Thus, this may be concluded that at room temperature the coexistence of two phases (one monoclinic and second of higher symmetry) is possible. The last phase is most probably metastable and is related to the fixed paraelastic phase on structural defects. The mechanical switching of domains was experimentally confirmed so it supports the ferroelastic character of the described phase.

On cooling, DMACB undergoes the transition (IV→V) to a new phase which is evidenced by preliminary X-ray investigations. This is accompanied by an appearance of a large amount of small domains with walls parallel to the ***a***-axis as well as by W' walls tilted to ***a***-axis. We did not succeed in determination of optical parameters of this new phase due to the small size of domains and visible strains. The subsequent

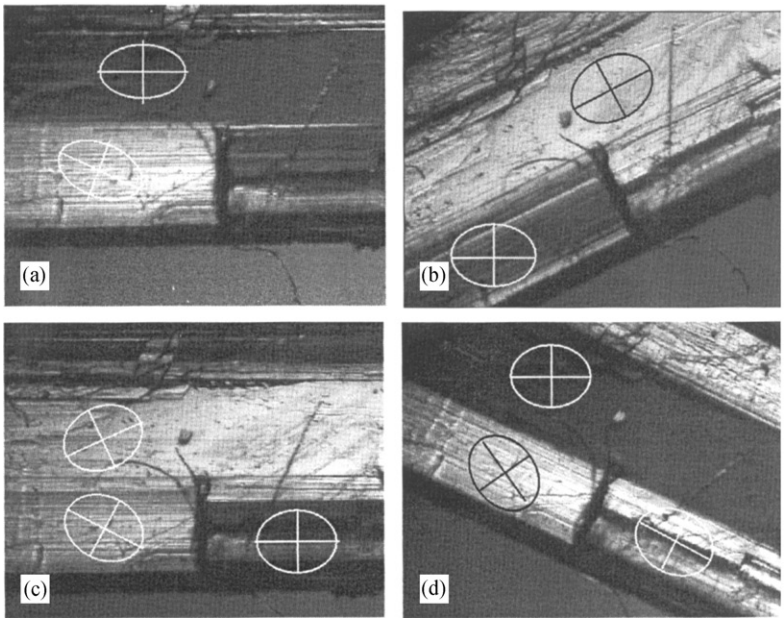

Fig. 7. Coexistence of the phases and ferroelastic switching for the DMACB crystal: (a) and (b) before switching; (c) and (d) after switching ($T = 298$ K). The visible edge of crystal is parallel to the ***a***-axis. The visual field is about 1 mm^2.

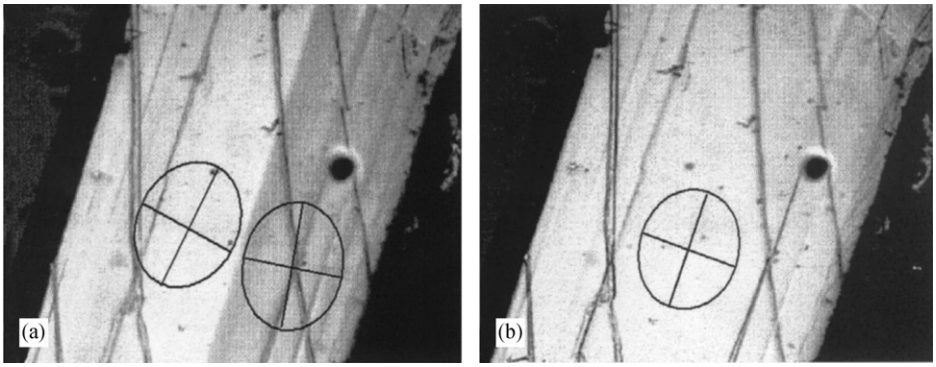

Fig. 8. Ferro-paraelastic phase transition in DMACB at 363 K. (a) The ferroelastic domain structure below 363 K (b) the paraelastic phase at 364 K.

phase transitions (on heating) lead only to some rebuilding of domains, but due to the complex picture, this situation was not analyzed in details. The optical observations of the crystal with polarizing microscope indicate that the structural phase transition at 363 K (see Fig. 8a and b) leads to a paraelastic phase (phase I). That is clearly confirmed by the disappearance of the ferroelastic domain structure (Fig. 8b). Thus the paraelastic phase I has at least the orthorhombic symmetry.

We succeeded in the birefringence measurements performed only for cleaved samples (along the ***b***-axis). These results may be treated only quantitatively due to the occurrence of very narrow domains. The dependence of Δn_b versus temperature is shown in Fig. 9. Only two discontinuous phase transitions at 285 and 363 and one continuous at 340 K might be identified.

3.5. The vibrational spectra

Since the additional phase transitions in DMACB were postulated by Rajan et al. [13] (at 150 and 78 K) we performed temperature dependent IR studies down to 40 K. We wanted to check whether the possible phase transitions involved any changes in the IR spectra of DMACB.

FT-IR technique is not the best method for detection of phase transitions, nevertheless when the phase transition is due to the change in dynamical state of molecules, it is usually reflected in anomalies in positions and half-width of the corresponding absorption bands.

The temperature-dependent IR studies on the powder samples of various dimethylammonium halogenoantimonates(III) and bismuthates(III) were already

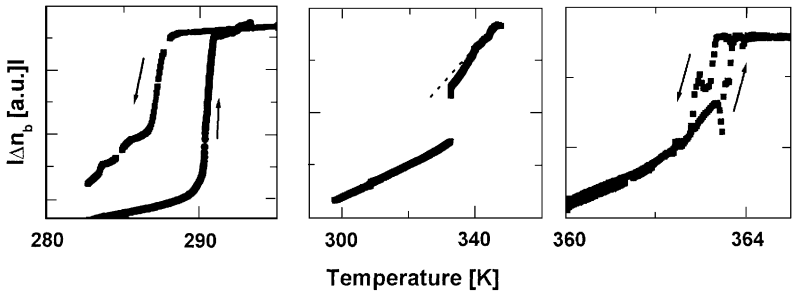

Fig. 9. Temperature dependence of the linear birefringence Δn_b for the DMACB crystal.

performed for the internal modes of the dimethylammonium cations (3600–400 cm^{-1}) [20]. It has turn out that the most sensitive vibrations to the structural phase transition appeared to be the symmetric and asymmetric NC_2 stretching modes. This confirmed a contribution of the changes in the vibrational state of the methylammonium cations to the mechanism of the transitions. The bands assigned to the $\nu(NC_2)$ vibrations are observed between 1000 and 1025 cm^{-1} (asymmetric) and between 875 and 895 cm^{-1} (symmetric). Therefore we decided to limit a temperature analysis of powdered spectra of DMACB to these wavenumber regions. The FT-IR spectra have been collected at temperatures ranging between 40 and 300 K. As an illustration Fig. 10 presents the evolution of the spectra in the range between 1000 and 1025 cm^{-1}.

At room temperature only single symmetric broad bands are visible in the stretching symmetric and asymmetric CN vibrations region of the DMA group, whereas at the lowest temperature at least 3 to 4 bands may be distinguished in the corresponding frequency regions (see Fig. 11a and b). The splitting observed at low temperature appears as a result of at least two effects. The first effect is related to the splitting of broad bands associated with the reduction of freedom for rotation of cations. Another effect is connected with the differentiation of cations in the crystal lattice, since the phase transitions lead to lowering of the crystal symmetry. It is difficult to separate these two effects. From the presented above results of the X-ray studies it is known that at the 285 K phase transition the symmetry of the DMACB crystal changes from monoclinic to triclinic. It should be stressed that in DMACB the step-wise splitting of the bands takes place at 285 K. This confirms the supposition that the dynamics of DMA cations changes at this temperature and contributes to the mechanism of the 285 K phase transition.

From Fig. 11a and b it is clear that we deal with very rigid structures and no changes are observed in the IR spectra between 40 and 150–160 K. This, in our opinion, excludes rather any structural transformation postulated at 78 K by Rajan et al. [13]. It should be noticed,

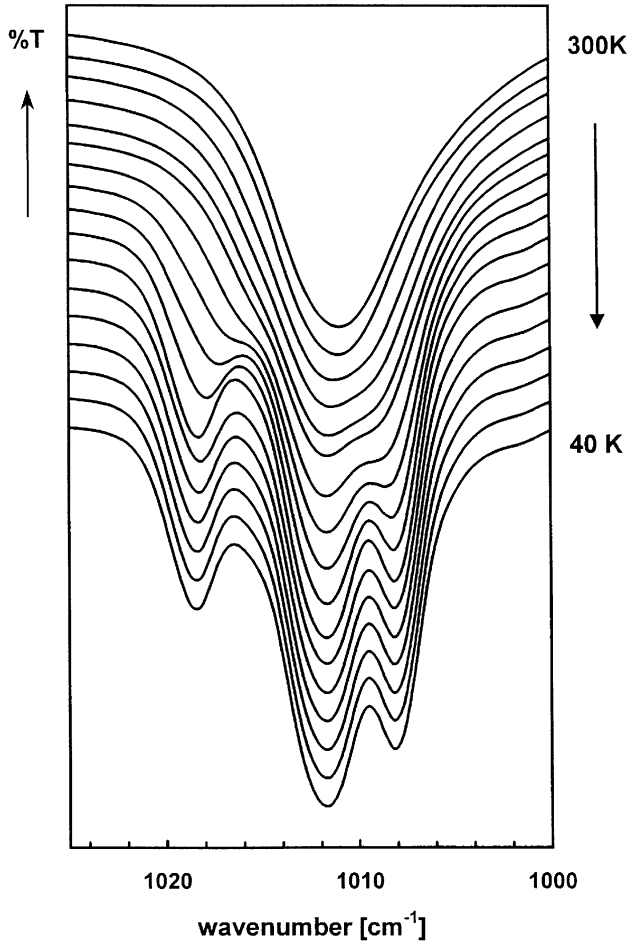

Fig. 10. Temperature evolution of the spectra in the region of the asymmetric $\nu(NC_2)$ vibrations between 40 and 300 K. Between 300 and 240 K the spectra were recorded every 10 K, and between 240 and 40 K every 20 K.

however, that the some small changes in the IR spectra are really observed in the temperature region above 150–160 K, i.e. in a region where the second phase transition was observed by Rajan et al. [13]. The gradual shifts of the bands is observed in this temperature range which may be explained by a change in the dynamical state of DMA cations.

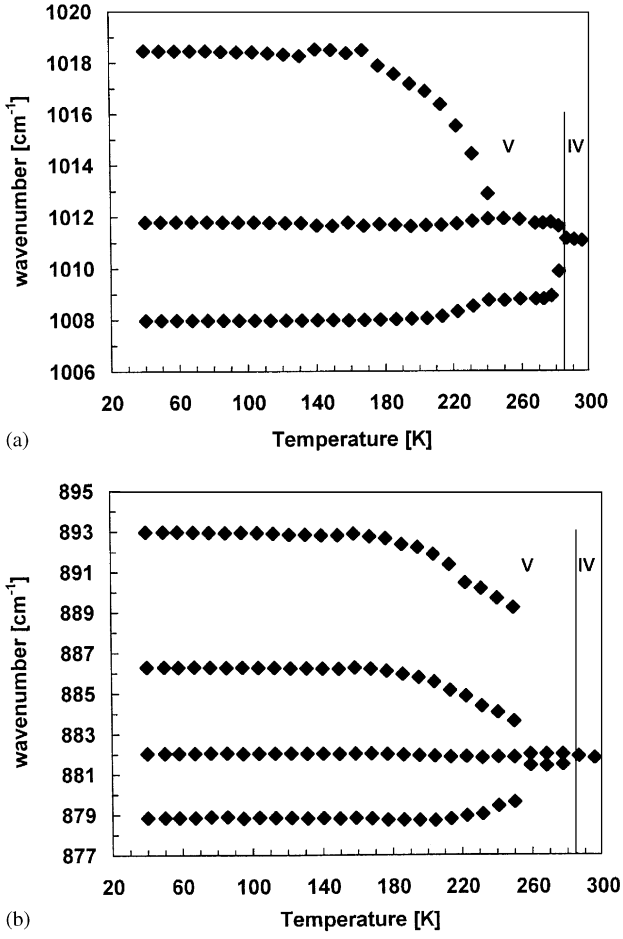

Fig. 11. (a) Temperature dependence of the frequencies of the asymmetric $\nu(NC_2)$ vibrations between 1020 and 1006 cm^{-1} and (b) symmetric $\nu(NC_2)$ modes between 877 and 895 cm^{-1}.

4. Discussion

The presented above results of studies indicate the following sequence of phase transitions in DMACB:

phase	V	IV	III	II	I
symmetry	triclinic	monoclinic incommensurate	(?)	monoclinic $P2_1/n$	orthorhombic(?)
T_c/K (cooling/heating)	285/292		323/325	340/341	367/369

It seems interesting to compare the phase situation in DMACB proposed by us to that reported by Rajan et al. [13]. Their ^1H NMR data point out two structural phase transitions in the low-temperature region, namely, at 152 and 78 K.

Our investigations based on the results of techniques fundamental for detection of phase transitions, the differential scanning calorimetry, dilatometry and dielectric measurements, rule out the possibility of an existence of any phase transitions in the vicinity of 152 K. The existence of the suggested phase transition at 78 K remains still open. Nevertheless the subtle changes in the present IR spectra below 160 K may reflect a change of the dynamics of the CH_3 groups seen in the NMR measurements reported by Rajan et al. [13]. In series of crystals containing alkylammonium cations one usually observes the freezing of CH_3 motions in the temperature region 150–100 K. On the other hand it is known that the freezing of the C_3 type motion of the methyl group does not lead to any change in the symmetry of the crystal, so in consequence it cannot be connected to the phase transition.

The main conclusion resulting from our studies is that there are four phase transitions in DMACB between 280 and 400 K and no phase transitions in the low-temperature region down to 40 K. It means that the sequence of phase transition proposed in this paper is quite different from that reported by Rajan et al. [13].

Moreover the model of dynamics of DMA cations proposed by authors in [13] seems to be in disagreement with that found by the X-ray and dielectric studies. Their model assuming the isotropic rotation of 50% DMA cations even below 350 K is not confirmed by present X-ray results.

Dynamic properties of the DMACB crystal should be discussed on the basis of both X-ray and dielectric results. There is no doubt that the motion of organic cations plays the main role in all phase transitions mechanisms. The presented dielectric studies show that at 323 and more clearly at 285 K phase transitions a rapid freezing of the reorientation of dipolar groups (DMA) takes place. We should notice that the C_2 type reorientation of the cations cannot contribute to the dielectric increment because it is not accompanied by a change in resultant dipole moment of the unit cell. The dielectrically active motion should be connected with the displacement of the N atom with respect to the anionic sublattice. We suggest an analogy between the motion of the $[(CH_3)_2NH_2^+]$ cations and the reorientation of this dipolar group in widely studied ferroelectrics, $[(CH_3)_2NH_2]_3[Sb_2Cl_9]$ [19] and $[(CH_3)_2NH_2]_3[Sb_2Br_9]$ [11]. The only motion contributing to the electric permittivity is the reorientation around the C–C axis of the cation involving the shift of the N atom. The lack of the dielectric dispersion up to 1 GHz indicate

relatively fast reorientation of these cations with the relaxation times shorter than 1×10^{-9} s.

The comparison of the physical and structural properties of $[(CH_3)_2NH_2]_3[Sb_2Cl_9]$ and $[(CH_3)_2NH_2]_3[Bi_2Cl_9]$ may be instructive. Recently we studied the phase situation in mixed crystals $[(CH_3)_2NH_2]_3[Sb_{2(1-x)}Bi_{2x}Cl_9]$ [21]. It was shown that substitution of Sb by Bi atoms, first of all, modifies the anionic sublattice. For the $x \geqslant 0.17$ the two-dimensional polyanionic structure $[M_2Cl_9^{-3}]_n$ anions is replaced by the double chains of polyhedra. This is directly connected with the disappearance of ferroelectric properties.

In conclusion we can state that the appearance of polar properties for the chloroantimonate(III) and chlorobismuthate(III) with the $R_3M_2X_9$ composition requires the presence of two-dimensional polyanionic layers in the crystal structure.

Acknowledgments

This work was supported by the Polish State Committee for Research (project register number 7 T09A 070 21).

References

[1] R. Jakubas, L. Sobczyk, Phase Transitions 20 (1990) 163.
[2] L. Sobczyk, R. Jakubas, J. Zaleski, Polish J. Chem. 71 (1997) 265.
[3] H. Ishihara, K. Watanabe, A. Iwata, K. Yamada, Y. Kinoshita, T. Okuda, V.G. Krishnan, S. Dou, A. Weiss, Z. Naturforsch. 47a (1992) 65.
[4] T. Kawai, E. Takao, S. Shimanuki, M. Iwata, A. Miyashita, Y. Ishibashi, J. Phys. Soc. Japan 68 (1999) 2848.
[5] J. Jóźków, R. Jakubas, G. Bator, A. Pietraszko, J. Chem. Phys. 114 (2001) 7239.
[6] R. Jakubas, Z. Czapla, Z. Galewski, L. Sobczyk, O.J. Żogał, T. Lis, Phys. Status Sol. a 93 (1986) 449.
[7] A. Kallel, J.W. Bats, Acta Cryst. C41 (1985) 1022.
[8] B. Chabot, E. Parthe, Acta Cryst. B34 (1978) 645.
[9] G. Bator, R. Jakubas, J. Zaleski, J. Mróz, J. Appl. Phys. 88 (2000) 1015.
[10] R. Jakubas, Solid State Commun. 60 (1986) 389.
[11] J. Zaleski, Cz. Pawlaczyk, R. Jakubas, H.-G. Unruh, J. Phys.: Condens. Matter 12 (2000) 7509.
[12] M. Bujak, J. Zaleski, Cryst. Eng. 4 (2001) 241.
[13] P.K. Rajan, B. Jagadesh, K. Venu, V.S.S. Sastry, Solid State Commun. 100 (1996) 519.
[14] KUMA Diffraction Software, version 10.1.11, KUMA Diffraction, Wrocław, Poland 1999.
[15] G.M. Sheldrick, SHELXS-97. Program for the Solution of Crystal Structure, University of Göttingen, Germany, 1997.
[16] G.M. Sheldrick, SHELXL-97. Program for the Refinement of Crystal Structure, University of Göttingen, Germany, 1997.
[17] G.M. Sheldrick, SHELXTL Siemens Analytical X-ray Instruments Inc., Madison, Wisconsin, USA, 1990.
[18] G.A. Landrum, R. Hoffmann, Angew. Chem. Int. Ed. 37 (1998) 1887.
[19] J. Zaleski, A. Pietraszko, Acta Cryst. B 52 (1996) 287.
[20] R. Jakubas, G. Bator, J. Baran, J. Phys. Chem. Solids 54 (1993) 1065.
[21] M. Wojtaś, G. Bator, R. Jakubas, J. Zaleski, J. Phys.: Condens. Matter 13 (2001) 8831.